Creep Deformation Characteristics of Weathered Granite

AUTHOR(S):

AKAI, Koichi; ADACHI, Toshihisa; YAMAMOTO, Kazuo; OHNISHI, Yuzo

CITATION:

AKAI, Koichi ...[et al]. Creep Deformation Characteristics of Weathered Granite. Memoirs of the Faculty of Engineering, Kyoto University 1977, 39(1): 183-200

ISSUE DATE:

1977-03-31

URL:

http://hdl.handle.net/2433/281028

Creep Deformation Characteristics of Weathered Granite

By

Koichi AKAI*, Toshihisa ADACHI**, Kazuo YAMAMOTO***
and Yuzo OHNISHI*

(Received September 30, 1976)

Abstract

Creep deformation characteristics of weathered granite were studied. While displacement of a structure on foundation rock is the main concern of foundation designers, the mechanical and especially the time dependent properties of weathered granite, which is being used recently as a foundation rock in Japan, have not been investigated so much.

The test results show that the behavior of soft rock is very similar to that of soil. The time dependent deformation in soft rock can be predicted by a simple stress-strain-time function or rheological models. The time to failure under a sustained creep load was also discussed in relation to the strength of weathered granite.

1. Introduction

The problem of designing a foundation on rock is substantially the problem of predicting the load-deformation response of a given site. Given this information, an engineering solution is always possible: either the structure can be designed to suit the predicted load-deformation response, or the properties of the foundation rock can be changed artificially, say, by grouting or pre-stressing.

Predictions of the load-deformation response require mainly the mechanical properties of the rock and rock mass. Establishng the mechnical properties of the rock mass requires laboratory testing to determine the rock substance properties as well as field investigations to determine the in-situ stress, groundwater and geologic

* Department of Transportation Engineering
** Disaster Prevention Research Institute
*** Osaka Prefectural Technical College

conditions of the site.

It is traditional, in civil engineering, to consider that there are two criteria of failure: excessive displacement and total collapse. These criteria are reflected in the current methods of analysis (limit analysis, dealing with a total collapse without any consideration of displacement, and stress displacement analysis with only the consideration of local failure). In a foundation design on rock, there is substantially only one criterion of "failure", i. e., excessive displacement. This concept of displacement as the sole criterion of failure is of particular value today when analytical techniques such as finite element methods exist for simulating displacement behavior.

Rock shows time-dependent and time-independent deformations. The time-dependent deformation known as creep is very important especially for soft rock such as weathered granite, mud stone, etc., which have often been used for foundations recently in Japan. Unfortunately, the study on the mechanical behavior of such kinds of rock has not been done sufficiently.

In this paper, three types of weathered granite which belong to the C_L-D_L class in rock classification were tested in a laboratory in order to investigate the strength and deformation characteristics of these soft rock specimens. Emphasis is on the stress-creep deformation behavior of rock, rather than on the strength parameters, which are reported in an other paper[1].

The results obtained from triaxial compression and creep tests were discussed in relation to the behavior of soil materials. In the following, a review of the general characteristics of the strength and stress-strain-time behavior of weathered granite and creep rupture are treated in detail.

2. Material Properties of Weathered Granite

Three different types of weathered granite have been tested in the laboratory in order to investigate the strength and creep deformation characteristics. As shown in Table 1, the specimens Sample I are heavily weathered and the mineral ingredients have changed to clay. Therefore, cracks and discontinuities are not found at all. The specimens in Sample II are not weathered so much as those in Sample I and have crystalline minerals which still hold large grain sizes. They are very fragile and can not stand by themselves in water without confinement. The specimens in Sample III are the strongest among the three sample groups, and they can be sampled by a diamond core cutter. Cracks and discontinuities exist in the specimens, and they may control the mechanical behavior of the sample.

The porosity of a rock is a good index to know the degree of weathering and to estimate the property of the rock. Therefore, the porosity of weathered granite was carefully measured, and it was found that it was closely related to its strength

Table 1. Physical Properties of Weathered Granite

Sample	I	II	III
n' (%)	35	18	6
γ (g/cm^3)	1.65	2.14	2.45
Gs	2.60	2.61	2.65
Sr (%)	90.0	75.0	95.0
Hardness or Softness	Heavily weathered. Decomposed to clay. Cracks are not noticeable.	Some of quartz and feldspar mineral grains are not weathered. Very fragile	Sampleable by a diamondc ore cutter. Cracks exist.
Rock Classification	D_L	D_M	C_L

and deformability. However, it is extremely difficult to make test specimens for triaxial tests from those fragile weathered rocks whose porosity is more than 10%. This is why the mechanical properties of such rock were not known at all. In this study, we made a breakthrough in overcoming this difficulty by special techniques[1] and obtained useful experimental data.

3. Strength Parameters

The strength of rock has been the main concern of engineers who work with rocks. However, the definition of failure has been changed, and therefore design procedures must be pursued in considering the deformation and the longterm stability of rock masses.

Recently, we proposed the following two methods for soft rock by defining the strength parameters from the triaxial compression and the triaxial creep test data[1].

(i) When a stress-strain curve is plotted in a log-log scale, it is approximated by two lines broken at a yield point (designated as Y), as shown in Figs. 1(a) and 1(b). It is generally known that stable micro-cracks are created at this yield stress level, and a failure of the rock structure would occur if a load which is more than this level were to be continuously applied.

(ii) The volume of a rock specimen subjected to a deviator stress, in a drained condition, usually contracts at the beginning, and after reaching the minimum point it expands due to dilatancy. Under an undrained condition, the induced pore pressure shows a similar behavior because the volume of the specimen is kept constant. The point of the minimum volume or the maximum pore pressure is designated by M, and physically it is explained that it is at such a point where the unstable cracks

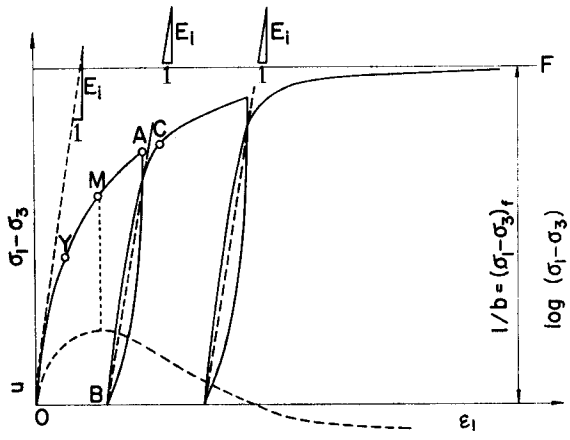

Fig. 1 (a). Stress-Strain Relationship with Change of Induced pore Pressure

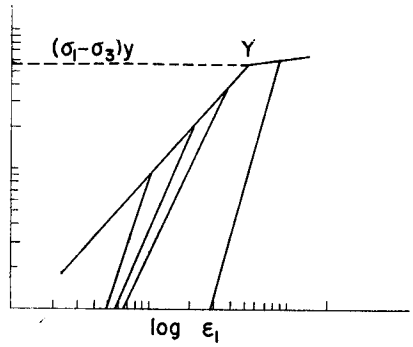

Fig. 1 (b). Log Stress-Log Strain Relationship

are to be generated and the internal grain structure of the specimen is drastically changed.

Table 2 shows the strength parameters of the Mohr-Coulomb type failure criterion calculated from point Y and M for Samples I and II. The strength test for Sample III was not sufficiently carried out and there was not enough information to derive the strength parameters. The uniaxial strength for Sample III was more than 50 kg/cm^2. Fig. 2 shows the comparison of the results by Onodera, et al[2]. with our own results. Although their tests are mainly on specimens whose properties are less than 10%, our results for the angle of friction ϕ' are reasonable. It is seen that cohesion c' is greatly affected by the degree of weathering.

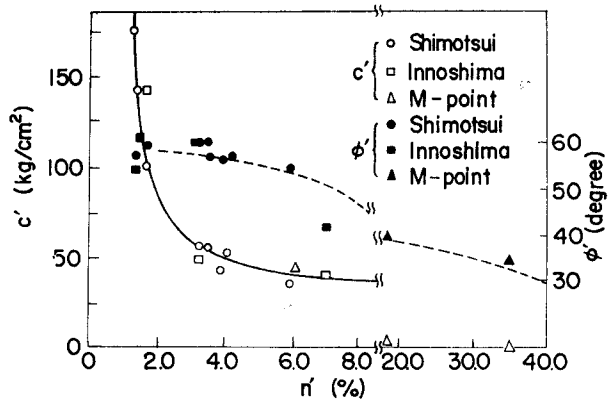

Fig. 2. Effect of Porosity on Internal Friction Angle and Cohesion of Granite

Table 2. Strength Parameters of Weathered Granite

Sample		c'	ϕ'
I	Y	0	21.6°
	M	0	35.3°
II	Y	0	34.9°
	M	0.6	37.7°
	F	2.64	44.8°

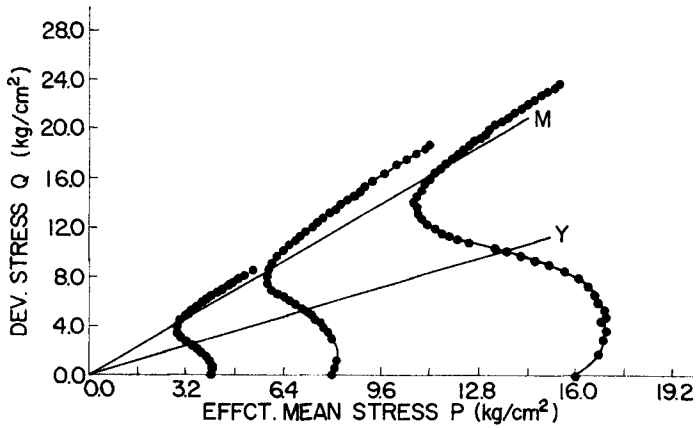

Fig. 3. Stress Paths, and Yield and Failure Lines of Weathered Granite in Triaxial Shear Test

The stress paths of triaxial shear tests, yield line (line of point Y) and failure line (line of point M) for the specimens of Sample I, for example, are shown in Fig. 3. Most of the rock specimens in Samples I, II and III show a very similar behavior. They show a strain-hardening or a strain-softening behavior according to a low or high initial confining (consolidation) pressure.

4. Creep of Weathered Granite

4.1 General Characteristics

The time-dependent responses of soft rock may assume a variety of forms, depending on such factors as the rock type, structure, stress history, drainage conditions, type of stress system and other factors. In many cases, application of a stress leads first to a period of transient creep, during which the strain rate decreases continuously with time, followed by creep at a constant rate for some period (steady state). For materials susceptible to a creep rupture, the steady state period is followed by an accelerated creep rate leading to failure as shown in Fig. 4.

In order to estimate the complex creep behavior of geologic materials for use in practice, a rheological model approach and an empirical relationship method have been proposed. Rheological models have been developed in an effort to duplicate the stress-strain-time response of a material in terms of various arrangements of springs, dashpots and sliders. Alternatively, it has been shown that the relationships between the strain rate, stress and time make possible the use of simple expressions for the characterization of creep. Phenomenological relationships developed by both methods are curve-fitting techniques that do not necessarilly imply anything about the

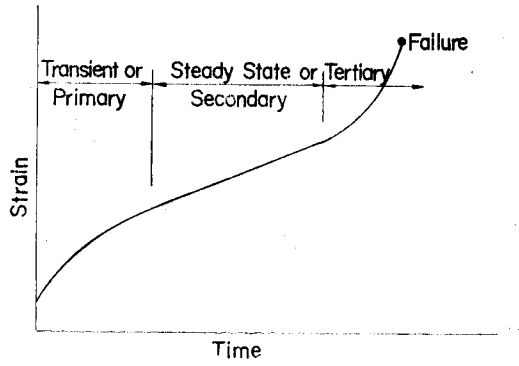

Fig. 4. Stages of Creep

mechanisms underlying the deformation process.

We will explain and discuss the two methods in relation to the behavior of weathered granite, and will find the useful stress-strain-time relationships in practice.

4.2 Rheological Models

Different rheological models have been proposed for a mathematical description of the stress-strain-time behavior of rocks and soil specimens, for example, Murayama and Shibata[3], Christensen and Wu[4], and Komamura and Huang[5]. Here, we will propose five-element Voight type rheological models for the different levels of

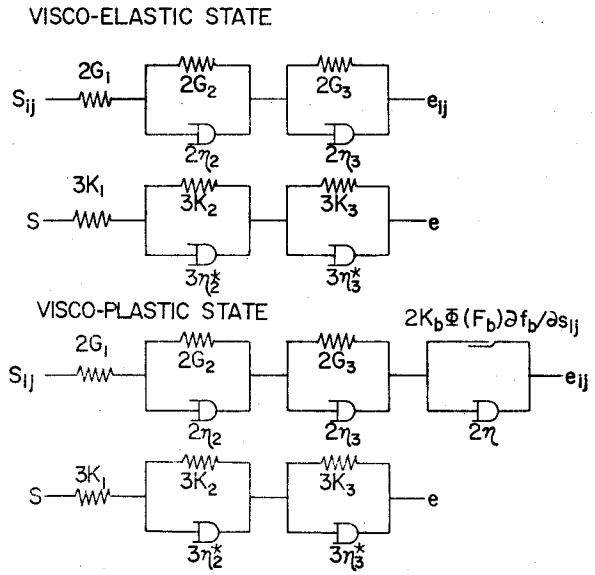

Fig. 5. Five Elements Rheological Models

stress in soft rock, as shown in Fig. 5. The symbols used in the figure are explained as follows.

Deviator stress	: $s_{ij}=\sigma_{ij}-\sigma_{kk}\delta_{ij}/3$
Mean stress	: $s=\sigma_{kk}/3$
Deviator strain	: $e_{ij}=\varepsilon_{ij}-\varepsilon_{kk}\delta_{ij}/3$
Volumetric strain	: $e=e_{kk}$
Strain hardening parameter	: k
Excess stress function	: F
Dynamic yield function	: f_d
Material constants	: $G_1, G_2, G_3, K_1, K_2, K_3, \eta_2, \eta_3, \eta, \eta_2^*\eta_3^*$

Mathematical relationships can be derived for these models as follows:
For a visco-elastic state,

$$e_{ij}=s_{ij}(t)/2G_1+(1/2\eta_2)\int_0^t e^{-(G_2/\eta_2)(t-\tau)}s_{ij}(\tau)d\tau + (1/2\eta_3)\int_0^t e^{-(G_3/\eta_3)(t-\tau)}s_{ij}(\tau)d\tau \quad (1)$$

$$e=s(t)/3K_1+(1/3\eta_2^*)\int_0^t e^{-(K_2/\eta_2^*)(t-\tau)}s(\tau)d\tau + (1/3\eta_3^*)\int_0^t e^{-(K_3/\eta_3^*)(t-\tau)}s(\tau)d\tau$$

Under a condition of constant stress, $s_{ij}(t)$=constant. Therefore, differenciating by time t, Eq. (1) becomes

$$\partial e_{ij}(t)/\partial t=\dot{e}_{ij}=\left[e^{-(G_2/\eta_2)t}/2\eta_2+e^{-(G_3/\eta_3)t}/2\eta_3\right]s_{ij}(t)$$

$$\partial e(t)/\partial t=\dot{e}=\left[e^{-(K_2/\eta_2^*)t}/3\eta_2^*+e^{-(K_3/\eta_3^*)t}/3\eta_3^*\right]s(t) \quad (2)$$

For a visco-plastic state,

$$\dot{e}_{ij}=\left[e^{-(G_2/\eta_2)t}/2\eta_2+e^{-(G_3/\eta_3)t}/2\eta_3\right]s_{ij}(t)+(k/\eta)\phi(F)\partial f_d/\partial s_{ij}$$

$$\dot{e}=\left[e^{-(K_2/\eta_2^*)t}/3\eta_2^*+e^{-(K_3/\eta_2^*)t}/3\eta_3^*\right]s(t) \quad (3)$$

In this section, we will only consider a visco-elastic state, while a visco-plastic stress state will be briefly discussed later in relation to creep rupture.

In the case of a triaxial creep test, a specimen is cylindrical and then its stress and strain are:

$$s_{11}=2(\sigma_1-\sigma_3)/3, \quad s=(\sigma_1+2\sigma_3)/3$$

$$e_{11}=2(\varepsilon_1-\varepsilon_3)/3, \quad e=\varepsilon_1+2\varepsilon_3$$

Eq. (2) is deduced to:

$$\dot{e}_{11}/s_{11}=\left[e^{-(G_2/\eta_2)t}/2\eta_2+e^{-(G_3/\eta_3)t}/2\eta_3\right] \quad (4)$$

A plot of $\log(\dot{e}_{11}(t)/s_{11})$ vs. time in a triaxial creep test of soft rock usually yields a

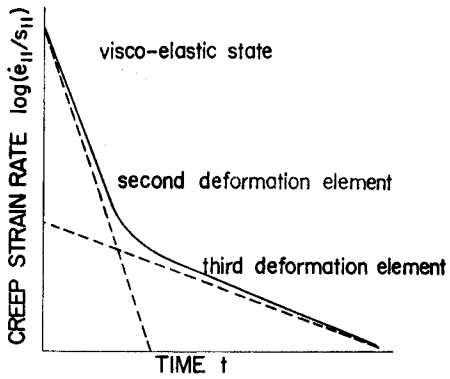

Fig. 6. General Relationship between Log Creep Strain Rate and Time

curve as shown in Fig. 6. Here, if it is assumed that the first term on the right hand side in Eq. (4) (corresponding to the second deformation element in the model) mainly describes the behavior of the creep deformation of the rock when time t is relatively small, and the second term (third deformation element) similarly describes its behavior when time t is large, two straight lines are approximately drawn as seen in Fig. 6, and the material constants η_2, η_3, G_2, G_3 can be determined. The values of η_2 and η_3 are obtained from the intersections of the vertical axis where t=0 and two approximated straight lines. The slopes of these two lines yield the values of G_2/η_2 and G_3/η_3. The instantaneous elastic modulus G_1 is determined from the amount of instantaneous deformation and the load increment.

For the relationship between the mean stress and the volumetric strain, the material constants in Fig. 5 can be obtained similarly from an e-t curve. However, in this case, a special test in which only s is changed with a constant deviator stress or a test with a constant mean stress s is necessary. In practice, it can be assumed that the volumetric strain is only elastic since its time-dependency is very small, compared with the shear deformation in a visco-elastic state.

Fig. 7(a) shows a typical creep strain vs. time relationships with different stress levels for the specimens in Sample III. The same data plotted in the form of a logarithm of strain rate and time are shown in Fig. 7(b). It may be recognized that the relationship is well approximated by two straight lines, as seen in the figure. The instantaneous elastic modulus is obtained from a stress-strain curve in which the amount of creep strain was subtracted, as shown in Fig. 7(c). The behavior of creep deformation for Samples I and II is similarly described by the above model for Sample III. The calculated material constants for each sample group are listed in Table 3. It is known that if a rock is weak and soft, the values of its material

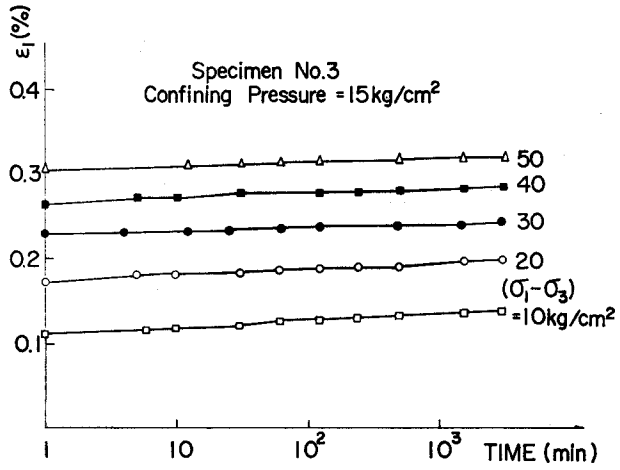

Fig. 7 (a). Strain-Time Relationships under Various Deviator Stresses of Sample III

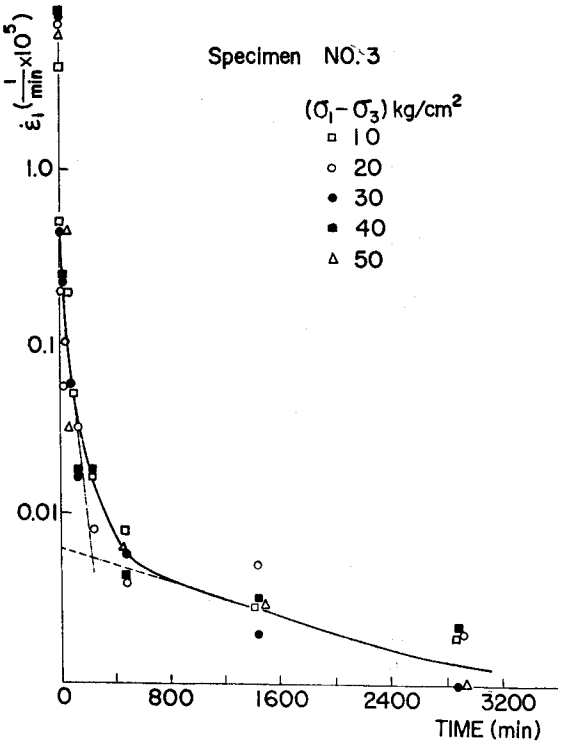

Fig. 7 (b). Log Strain Rate-Time Relationships of Sample III

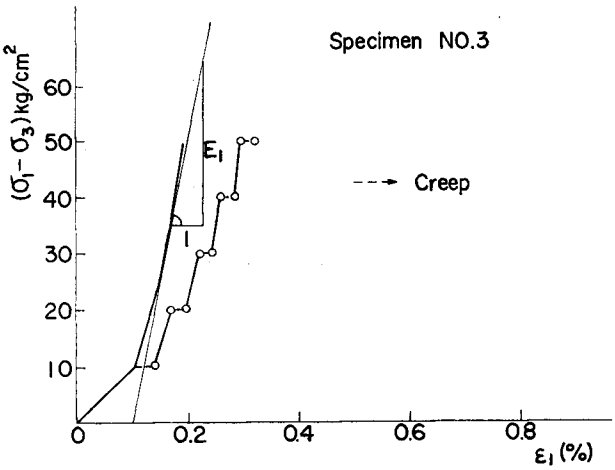

Fig. 7 (c). Determination of Instantaneous Elastic Modulus

Table 3. Material Contsants of Rheological Models

	Conf. pessr.	G_1	G_2	G_3	G_1^*	η_2	η_3	G_1^*/G_3	average
	kg/cm^2	kg/cm^2	kg/cm^2	kg/cm^2	kg/cm^2	kg • min./cm^2	kg • min./cm^2		
Sample I	2	2.6×10^2	2.7×10^3	1.3×10^2	4.2×10^2	9.3×10^3	4.7×10^5	0.32	0.21
	4	3.8×10^2	2.7×10^3	1.6×10^2	1.5×10^3	1.0×10^4	6.4×10^5	0.11	
	8	2.6×10^2	1.0×10^2	2.1×10^2	1.3×10^3	3.8×10^4	1.9×10^6	0.16	
	16	5.6×10^2	1.5×10^2	4.1×10^2	1.6×10^3	1.6×10^5	4.3×10^5	0.25	
Sample II	2	2.9×10^2	4.7×10^2	9.4×10^2	1.8×10^2	3.3×10^4	1.3×10^6	0.19	0.23
	4	4.7×10^2	9.9×10^2	1.5×10^3	3.2×10^2	8.0×10^4	1.5×10^6	0.21	
	8	1.1×10^3	1.7×10^3	2.5×10^3	6.6×10^2	2.4×10^5	7.4×10^6	0.27	
	16	2.6×10^3	2.4×10^3	5.2×10^3	1.3×10^3	4.6×10^5	1.6×10^7	0.24	
Sample III	2	6.2×10^3	2.8×10^4	4.7×10^4	5.1×10^3	2.2×10^6	1.6×10^8	0.11	0.12
	10	7.5×10^3	2.9×10^4	7.5×10^4	5.4×10^3	6.3×10^5	3.7×10^7	0.07	
	15	1.9×10^4	6.7×10^4	8.5×10^4	1.5×10^4	1.1×10^7	3.9×10^8	0.17	

constants are smaller and a larger deformation occurs with a smaller viscous resistance.

It is recognized that an increase in the confining pressure causes an increase in the deformation modulus of soil specimens and rocks. For cohesionless soil, the initial tangent, Young's modulus E_i, can be expressed by a relationship adapted from Janbu[6]

$$E_i = Kp_a(\sigma_c/p_a)^n \tag{5}$$

where K is a dimensionless modulus number, n is an exponent and P_a is a unit

constant equal to atmospheric pressure in the same units as the confining pressure σ_c. Similar variations of the material constants in the rheological model were observed. Therefore, we propose a similar equation in order to account for the effect of the confining pressure.

$$G_i = G_{0i} p_a (\sigma_c'/p_a)^n, \quad i=1, 2, 3 \tag{6}$$

where G_{01}, G_{02}, G_{03} are dimensionless numbers and σ_c' is an effective confining pressure. It was found that η_2, η_3 are not affected very much by the confining pressure. The values of the constants for Eq. (6) in each sample group are listed in Table 4.

Fig. 8 shows the instantaneous elastic modulus E_1 for these specimens of weathered granite. It was also found that E_1 decreased exponentially with an increase in porosity.

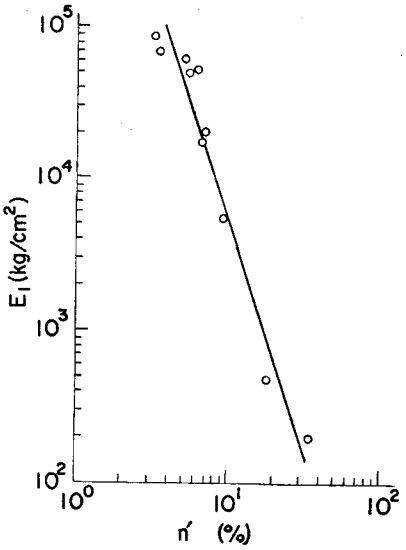

Table 4. Values of Material Constants, G_{01}, G_{02} and G_{03}

	G_{01}	G_{02}	G_{03}	n
	kg/cm^2	kg/cm^2	kg/cm^2	——
Sapmle I	1.0×10^2	2.0×10^2	3.2×10^2	0.55
Sample II	1.7×10^2	2.8×10^2	3.9×10^2	0.82
Sample III	4.8×10^3	2.1×10^1	3.7×10^1	0.32

←Fig. 8. Effect of Porosity on Instantaneous Elastic Modulud E_1

By using the above model, we could estimate the ratio of the total creep strain to the short-term strain, which is defined by a strain due to the first and second deformation elements. If it can be assumed that the deformation due to the second deformation element ceases in a short time with respect to the long-term deformation element ceases in a short time with respect to the long-term deformation of the third one, the first and second deformation elements are combined and replaced by a single deformation element like a spring. For example, the replaced elastic modulus G_1^* is written as:

$$G_1^* = G_1 G_2/(G_1 + G_2)$$

The ratio of the total creep strain to the short-term strain is given by G_1^*/G_3 and its value for each sample group is shown in Table 3. The ratio varies from about 0.1 to 0.3 depending on the rock strength, physical property, rock type, etc.. This simplified model method has proven to be very effective for soft rock species such as green tuff or rock salt since the long-term deformation can be easily predicted.

4.3 Empirical Stress-Strain-Time Functions

A characteristic relationship between the strain rate and time does exist for most soil, as illustrated by Fig. 9 (a) for a drained triaxial creep of London clay[7] and Fig. 9 (b) for an undrained triaxial creep of Osaka clay[8]. The same general pattern has been observed for weathered granite. A strain rate-time relationship of a specimen from Sample II tested under an undrained condition is shown in Fig. 10. At any stress level, the logarithm of the strain rate decreases linearly with the logarithm of time. The slope of this relationship is essentially independent of the creep stress, and increases in a stress shift with the line pointing vertically upwards. At stresses approaching the strength of the material, the strain rate becomes very large. The onset of failure is signalled by a reversal in the slope of the relationship, as shown in the figure.

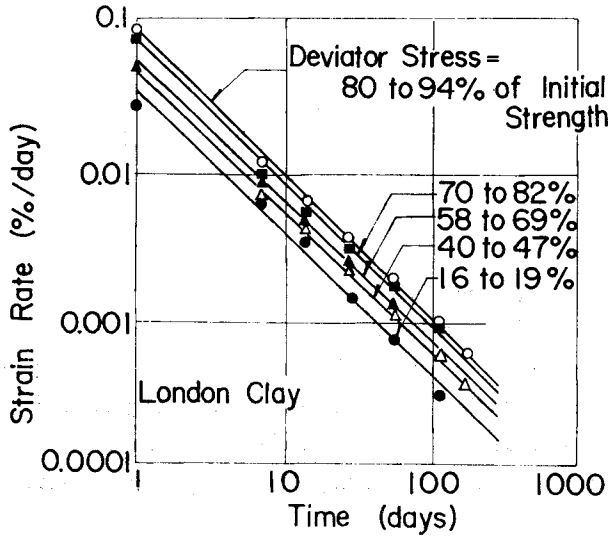

Fig. 9 (a). Strain Rate vs. Time Relationships during Drained Creep of London Clay (Data from Bishop, 1966)

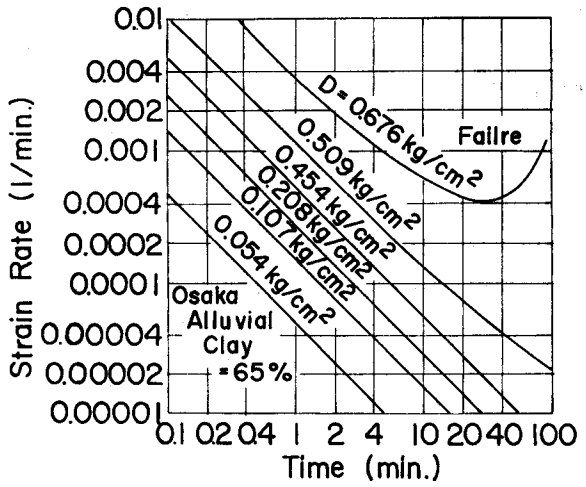

Fig. 9 (b). Strain Rate vs. Time Relationships durig Undrained Creep of Ostba Alluvial Clay (After Murayama and Shibata, 1958)

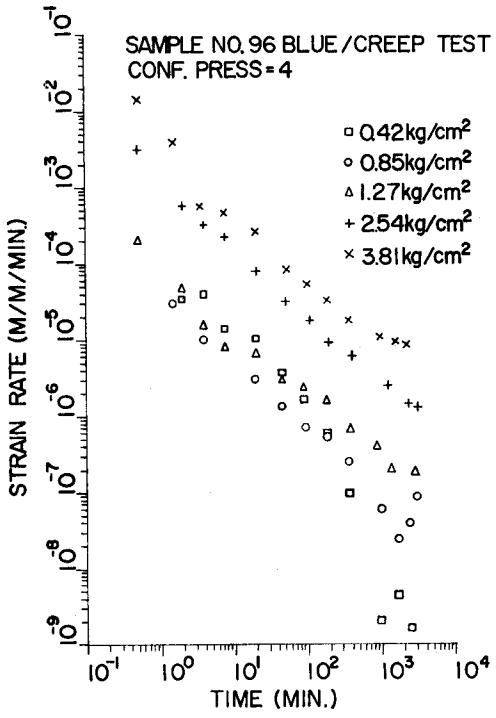

Fig. 10. Strain Rate vs. Time Relationships during Undrained Creep of Weathered Granit

Singh and Mitchell[9] have shown that the relationships between the strain rate $\dot{\varepsilon}$ and time t of the type illustrated in Figs. 9 and 10 could be expressed by

$$\dot{\varepsilon}=Ae^{\alpha D}(t_1/t)^m \tag{7}$$

where α denotes the slope of the linear part of the log strain rate versus the stress plot as illustrated in Fig. 11. D denotes a function of the stress intensity, m the absolute values of the slope of the straight line on the log strain rate vs. the log time plot, and t_1 a reference unit, for example, 1 min.. Here, the stress intensity D is taken as the deivator stress $(\sigma_1-\sigma_3)$. A is expressed by $\dot{\varepsilon}(t_1, D_0)$ which is the value of the strain rate obtained by projecting the straight line portion of the relationship between the log strain rate and the deviator stress at unit time to a value of D=0.

As seen in Fig. 10, we have found that most of our test results show m equals 1 or nearly equals 1. Since it is known that values of m generally fall in the range of 0.7 to 1.3, our result is quite reasonable. For the value of m equals 1, Eq. (7) is more simplified to:

$$\dot{\varepsilon}=Ae^{\alpha D}(t_1/t) \tag{8}$$

The calculated values of A and α for Samples I and II are listed in Table 5.

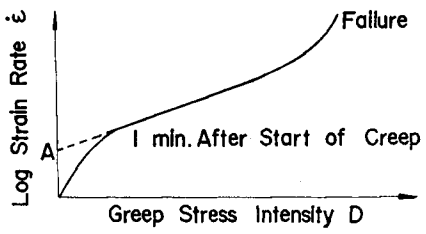

Fig. 11. Influence of Creep Stress Intensity on Creep Rate

Table 5. Creep Rupture Parameters of Weathered Granite

	σ'^c	α	A
	kg/cm²	1/kg/cm²	1/min.
Sample I	2	1.44	6.4×10^{-5}
	4	1.05	3.0×10^{-5}
	8	0.77	2.0×10^{-5}
	16	0.48	1.1×10^{-5}
Sample II	2	0.18	1.1×10^{-4}
	4		
	8	≒0.0	2.0×10^{-4}
	16		(1.0～3.0×10⁻⁴)

A general relationship between strain ε and time can be obtained by integration of Eq. (7).

If $\varepsilon=\varepsilon_1$ *at* $t=1$ and $t_1=1$,

$$\varepsilon=\varepsilon_1+Ae^{\alpha D}(t^{1-m}-1)/(1-m) \qquad \text{for } m\neq1 \tag{9}$$

$$\varepsilon=\varepsilon_1+Ae^{\alpha D}\ln t \qquad \text{for } m=1 \tag{10}$$

Eq. (10) sufficiently expresses the general creep behavior of weathered granite as shown in Fig. 7 (a).

From the data obtained in our investigation, it was recognized that the above

equation is applicable in the range of 30-90% of the peak strength; and is very effective and simple to estimate the amount of the long-term creep deformation.

4.4 Creep Rupture

Some soil and rock specimens may fail under a sustained creep stress significantly less (as much as 50%) than the peak stress measured in a normal triaxial shear test. The loss of strength as a result of creep may be explained in terms of the following principles of behavior[10]:

1) If a significant portion of the strength of a rock or a soil is due to cementation and creep deformations lead to a failure of the cemented bonds, then strength will be lost.
2) In the absence of chemical or rheological changes, strength depends on effective stresses at failure. If creep causes changes in effective stress, then strength changes will also occur.
3) In almost all soil and rock specimens, shear will cause changes in pore pressure in an undrained deformation, and changes in volume and water content in a drained deformation. Also, changes in water content cause strength changes.

In order to investigate changes in effective stress caused by changes in pore pressure during undrained creep loading, stress paths for specimens from Sample II are illustrated in Fig. 12. The Y line and M line are the yield line and the failure line, respectively, as discussed in Section 4.2. Tendencies of the stress paths generally resemble those of shear tests. At the end of the stress path, the specimen failed due to creep rupture. It was found, and should be noted, that while the creep strain

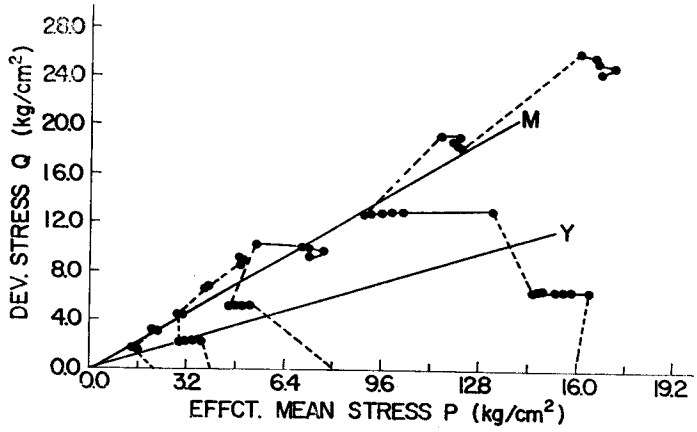

Fig. 12. Stress Paths of Weathered Granite during Undrained Creep Triaxial Test

converged in a short time at the stress level below the yield Y line, it became larger at the stress level beyond the yield line and eventually went into a steady state. Also, at around a point close to the failure M line, stress paths drastically change with a change in the induced pore pressure and rupture occurs in a short time.

For soft rocks susceptible to loss of strength, the time to failure is dependent on the stress level. In order to investigate creep rupture of weathered granite, the relationship between the load intensity $(\sigma_1-\sigma_3)/(\sigma_1-\sigma_3)_M$ and the minimum creep strain rate $\dot{\varepsilon}_s$ (corresponding to steady state strain rate) at the stress level where creep rupture occurs is plotted for Samples I and II in a semi-log scale, as shown in Fig. 13. The load intensity is normalized in dividing by the deviator stress at point M. It was found that the minimum strain rate $\dot{\varepsilon}_s$ prior to the onset of creep rupture decreased, and the time to failure increased for a given rock as the stress intensity decreased. This relationship is unique as may be seen by Fig. 14, which shows that

$$t_a=c/\dot{\varepsilon}_s$$

where c is a constant which depends on a material type, and t_a is the time when the accelerated creep strain is initiated. The values of c are about 0.02 and 0.001 for Samples I and Sample II, respectively. It is seen in the figure that a line generally shifts down to the left when the material becomes harder. This is known by the fact that if the material gets harder, it becomes more brittle and fails at a smaller

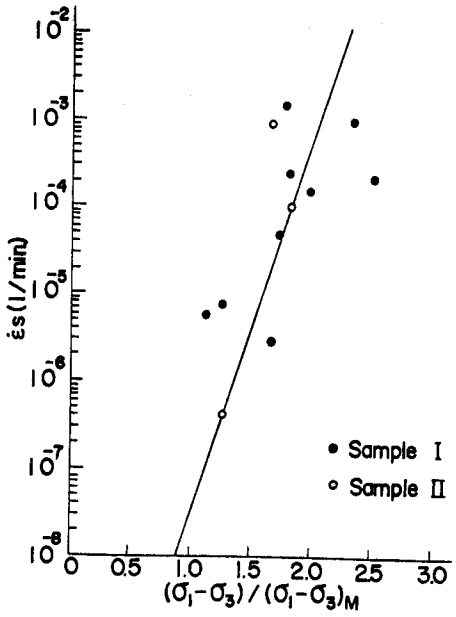

Fig. 13. Relationship between Liad Intensity and Minimum Creep Strain Rate

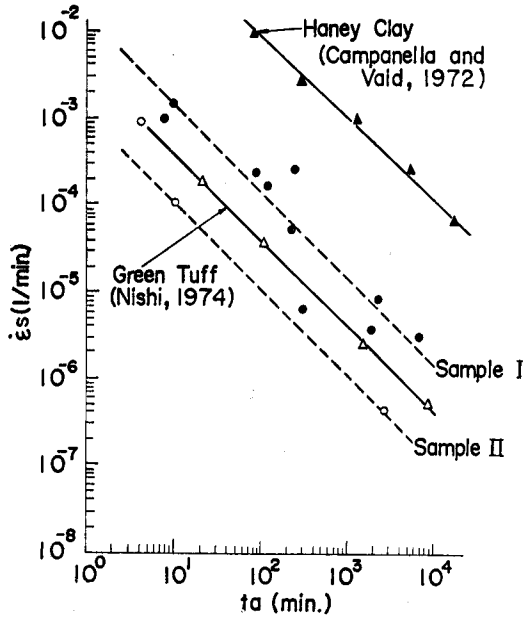

Fig. 14. Relationship between Time to Failure and Minimum Creep Rate

strain, as commonly noticed in the triaxial shear tests.

The total strain at which the accelerated creep strain was initiated is also found to be almost constant, independent of stress level, i. e. more or less 10% for Sample I and 5% for Sample II, which is same as the strain where the stress is at its peak in the triaxial shear test.

In this section, the phenomenon of creep rupture of weathered granite has been discussed only from the empirical point of view. Mathematically, this creep rupture may be represented by using a visco-plastic rheological model. In order to interpret all the data obtained in this study, however, some more detailed analyses and discussions are needed. We will present such analyses on an other occasion in a more elaborate form.

5. Conclusions

The strength and creep deformation characteristics of weathered granite were thoroughly studied in a laboratory, and the following conclusions were obtained:

(1) The behavior of soft rock such as weathered granite is very similar to that of soil.

(2) The strength parameters should be calculated from Y points for a long-term stability, and from M points for a short-term stability problem.

(3) Time-dependent deformations in soft rock follow predictable patterns and are essentially the same for all soft rock types. A simple three parameter stress-strain-time equation by Singh and Mitchell can be used to characterize the creep behavior of rock specimens. Rheological models are also useful.

Soft rock may fail under sustained stress as low as 50% of the strength in a conventional triaxial shear test. The strength changes can be accounted for in terms of changes in the effective stress, water content and matrix structure of specimens. The time to failure under a sustained creep load decreases with an increase in stress, and may be predicted by utilizing the empirical data.

References

1) Akai, K., Adachi, T., Yamamoto, K. and Ohnishi, Y.; Memoirs of Faculty of Engineering, Kyoto Univ. In Press (1976).
2) Onodera, T., Yoshinaka, R. and Oda, M.; Proceedings of 3rd Congress of I. S. R. M. (1974).
3) Murayama, S. and Shibata, T.; Proceedings of the Fifth International Conference on Soil Mechanics and Foundation Engineering, Vol. 1 (1961).
4) Christensen, R. W. and Wu. T. H.; Journal of the Soil Mechanics and Foundation Division, A. S. C. E., Vol. 90, No. SM6 (1964).
5) Komamura, F. and Huang, R. J.; Journal of the Geotechnical Engineering Division, A. S. C. E., Vol. 100, No. GT7 (1974).
6) Janbu, N.; European Conference on Soil Mechanics and Foundation Engineering, Wiesbaden, Germany, Vol. 1 (1963).
7) Bishop, A. W.; Geotechnique, Vol. 16 (1966).
8) Murayama, S. and Shibata, T.; Part 1, Bulletin No. 26, Disaster Prevention Research Institute (1958).
9) Singh, A. and Mitchell, J. K.; Journal of the Soil Mechanics and Foundation Division, A. S. C. E., Vol. 94, No. SM1 (1968).
10) Mitchell, J. K.; "Fundamentals of Soil Behavior", John Wiley & Sons (1976).